Quantification of human neutrophil motility in three-dimensional collagen gels

Effect of collagen concentration

Maria R. Parkhurst and W. Mark Saltzman
Department of Chemical Engineering, The Johns Hopkins University, Baltimore, Maryland 21218

ABSTRACT Leukocytes must migrate through tissues to fulfill their role in the immune response, but direct methods for observing and quantifying cell motility have mostly been limited to migration on two-dimensional surfaces. We have now developed methods for examining neutrophil movement in a three-dimensional gel containing 0.1 to 0.7 mg/ml rat tail tendon collagen. Neutrophil-populated collagen gels were formed within flat glass capillary tubes, permitting direct observation with light microscopy. By following the tracks of individual cells over a 13.5-min observation period and comparing them to a stochastic model of cell movement, we quantified cell speed within a given gel by estimating a random motility coefficient (μ) and persistence time (P). The random motility coefficient changed significantly with collagen concentration in the gel, varying from 1.6 to 13.3 $\times$ 10^{-9} cm^2/s, with the maximum occuring at a collagen gel concentration of 0.3 mg/ml. The methods described may be useful for studying tissue dynamics and for evaluating the mechanism of cell movement in three-dimensional gels of extracellular matrix (ECM) molecules.

INTRODUCTION

The ability of cells to migrate is critical to a variety of physiological phenomena, including tumor invasion and metastasis (Poste and Fidler, 1980), embryogenesis (Trinkhaus, 1984), angiogenesis (Folkman, 1985), and certain immune responses (Wilkinson and Lackie, 1979). The obvious significance of these events has motivated numerous studies into cell motility (Bellairs et al., 1982; Lackie, 1986), beginning with the seminal time-lapse studies of Comandon (1917). While recent studies have focused on the molecular mechanisms underlying cell movement (Sato et al., 1987; Ishihara et al., 1988; Sheetz et al., 1989; Cunningham et al., 1991), the influence of physical characteristics of the host tissue on cell motility is still largely unstudied, particularly in three dimensions. A more complete understanding of the influence of the extracellular environment on cell motility (particularly in environments that are similar to those found in vivo) would complement the molecular level studies. In addition, studies of cell behavior in different environments may lead to new methods for manipulating cell function or behavior in the body.

Most experimental methods for characterizing cell motility can be divided into two categories. In visual assays, the movements of a small number of cells are observed individually (Gail and Boone, 1970; Zigmond, 1977; Allan and Wilkinson, 1978). Population techniques require the observation of the collective movements of a group of cells (Boyden, 1962; Cutler, 1974; Nelson et al., 1975). A recent review outlines the experimental details of several specific assays and compares their advantages and limitations (Wilkinson et al., 1982). Both visual and population assays have been analyzed, enabling the quantification of intrinsic cell motility parameters (Gail and Boone, 1970; Dunn, 1983; Lauffenburger, 1983; Buettner et al., 1989; Farrell et al., 1990). One such parameter, the random motility coefficient (μ), characterizes the migration of cells in isotropic environments. Although each individual technique is self-consistent and reproducible, experimentally measured random motility coefficients can vary significantly between different assay systems (Buettner et al., 1989). This suggests that methods which mimic the host environment may be most useful for predicting cell behavior in vivo.

The most commonly used migration assays present cells with an environment that is much different from that encountered by cells in an organism. For example, many assay systems require cells to be attached to a two-dimensional substrate, while in tissues motile cells are frequently dispersed in three dimensions. Also, in most assays, motile cells contact glass, tissue culture polystyrene, or cellulose ester or acetate filters; the native extracellular matrix (ECM), however, is a complex gel of biopolymers, with collagen being the most abundant. In recent years, three-dimensional cell culture techniques have been developed to more closely

Address correspondence to Professor W. Mark Saltzman, Department of Chemical Engineering, The Johns Hopkins University, 3401 N. Charles Street, Room 42 New Engineering Building, Baltimore, MD 21218.

0006-3495/91/02/306/10 $2.00

simulate tissues (Elsdale and Bard, 1972; Bell et al., 1979; Schor, 1980; Schor et al., 1981; Richards et al., 1983). Of the few studies that have addressed cell motility in these situations (Schor et al., 1980; Brown, 1982; Haston et al., 1982; Wilkinson, 1985; Haston and Wilkinson, 1988; Wilkinson et al., 1988), most have involved plating a cell suspension on top of a collagen gel and subsequently following the infiltration of the gel by the cells. Most typically, infiltration is measured by following the leading front distance of the cell population as a function of time. While much information can be gained from these studies, the time course of the infiltration is usually on the order of hours or days. Furthermore, measurement of the leading front distance provides an accurate description of the behavior of the fastest moving cells rather than the entire cell population.

In this report, we present a new quantitative, visual assay for characterizing the migration of human neutrophils through collagen gels after direct encapsulation. In our experiments, cells move freely in three dimensions throughout the gel. However, because we monitor their migration through a conventional light microscope, the observed movements are two-dimensional projections of the actual movement (Fig. 1). Information about migration in the direction orthogonal to the microscope field is lost: an apparently stationary cell may actually be motionless or it may be moving perpendicular to the field of view. To recover this lost information, we compared our observations to a stochastic model of cell movement that quantitatively captures the two most important aspects of cell motility in isotropic environments: cells move randomly (they have no directional predispositions), and they do not usually move in straight lines for long times (persistence time is short). Using this model we can accurately reconstruct three-dimensional behavior from two-dimensional observations. We have used these experimental and analytical methods to determine the effect of collagen concentration on the random motility coefficient.

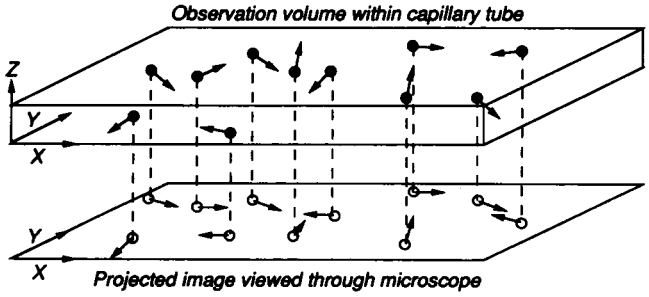

FIGURE 1 Schematic diagram of cell motility in a three-dimensional gel with observations within some microscopic field of view.

METHODS

Cell preparation

Whole blood from healthy donors was collected by venipuncture into vials containing heparin. Neutrophils were separated from whole blood samples via a standard technique (English and Andersen, 1974). Briefly, a solution of Ficoll in radiopaque media (Histopaque 1077, density = 1.077 g/ml; Sigma Chemical Co., St. Louis, MO) was layered onto an equal volume of a second Ficoll solution (Histopaque 1119, density = 1.119 g/ml; Sigma Chemical Co.). Heparinized whole blood was then layered onto the upper Ficoll solution, and the tubes were centrifuged at 700 *g* for 30 min. Cells were collected from the interface of the two Ficoll solutions and washed twice in phosphate buffered saline (PBS, pH = 7.4). Finally, the cells were suspended in PBS at $\sim 6 \times 10^6$ neutrophils/ml. The purity of the cell suspension was estimated by allowing 5 min for neutrophils to attach to the counting surface of a hemacytometer. During this time only neutrophils attached to the surface and, in this state, they were easily distinguished from unattached red blood cells. The attached cells were counted and the purity of the suspensions used ranged from 60 to 80% neutrophils, with the vast majority of remaining cells being erythrocytes. Other granulocytes (basophils and eosinophils) were not removed from the suspension; however, in healthy adult human blood these are present in such small numbers as to be statistically insignificant.

Collagen preparation and characterization

Solutions of type I collagen were prepared from rat tail tendons in a method similar to that of Bell et al. (1979). Tendons from the tails of 344 Fisher rats (250–300 g) (Harlan Sprague-Dawley, Indianapolis, IN) were extracted under 70% ethanol. The tendons were washed with fresh ethanol and placed in filter sterilized 0.02 M acetic acid ($\sim$100 ml solution/g wet tendon). Collagen from the tendons was allowed to solubilize in acetic acid for 2 d at 4°C. The mixture was then centrifuged at 18,000 *g* for 45 min, and the clear, collagen-containing supernatant was collected and stored as a liquid at 4°C. The concentration of collagen in the resulting solution was determined by (*a*) lyophilizing a measured volume of the solution and weighing the residual and (*b*) measuring total protein with a bicinchoninic acid assay (BCA protein assay; Pierce, Rockford, IL) using commercially prepared and purified type I collagen solutions from rat tail tendon (Collaborative Research, Bedford, MA) and calf skin (Boehringer Mannheim, Indianapolis, IN) as standards. The purity of the solution was confirmed by SDS-polyacrylamide gel electrophoresis.

Cell encapsulation

Neutrophils were encapsulated in type I collagen gels by a method similar to those previously reported for fibroblasts (Elsdale and Bard, 1972; Bell et al., 1979) and epithelial cells (Richards et al., 1983). First, the pH and osmolarity of the liquid collagen solution were raised to physiological levels (pH = 7.4; osmolarity = 300 mosM) by thoroughly mixing the following solutions in a microcentrifuge tube quickly and on ice: a predetermined amount of liquid collagen solution to obtain the desired final concentration in a final volume of 1 ml, a predetermined amount of 0.1 M NaOH so that the final solution pH was 7.4, 7 μl 5% (wt/vol) sodium bicarbonate, 100 μl 10× Media 199 (with Earle's Salts and L-Glutamine, without sodium bicarbonate; Gibco, Grand Island, NY), 40 μl 250 mM HEPES (Gibco), and a predetermined amount of highly purified water (18 MOhm resistance) to bring the final solution volume, including cells, to 1 ml. At this point, 125 μl of the neutrophil

suspension was added, and the solution was gently but thoroughly mixed by repeat pipetting. A small volume of this solution was drawn into a flat glass capillary tube (0.5 × 5.0 mm; Vitro Dynamics, Rockaway, NJ), which was then sealed and incubated at 37°C. The tube was left undisturbed for 7–10 min by which time the mixture had completely set. This protocol produced a neutrophil-populated collagen gel: type I collagen with neutrophils uniformly dispersed at a density of $\sim 7 \times 10^5$ cells/ml.

Cell motility assay

Experimental. A neutrophil-populated collagen gel was prepared inside a flat capillary tube as described above. Immediately after the 7–10-min gelation period, the tube was placed on the stage of an inverted light microscope (Diaphot; Nikon Inc., Garden City, NY). An incubator surrounding the stage was preheated and maintained at 37 ± 0.5°C throughout each experiment. Using a 20× phase contrast objective, a 0.3-mm² field of view was selected within the tube. Because the capillary tube was thick (~500 μm) compared with the depth of focus of the microscope objective (~50 μm), cells attached to the walls of the tube were easily distinguished from those moving freely in the gel. However, because cells were dispersed throughout the gel, choosing a focal plane was considerably more complicated than in conventional motility experiments, where cells are confined to a specific two-dimensional surface. In all cases, the field of view selected was at least 80 μm from any capillary tube surface as verified by the vertical focus micrometer. To assure that the gel was not excessively heated during the experiment, an infrared filter was placed in the path of the microscope light beam. In previous experiments, we confirmed that water in the focal plane remained at 37°C for 8 h (Saltzman et al., 1991).

A computer-based image analysis system (Compaq 386/20e with Data Translation 2851/2853 image acquisition and analysis boards, Houston, TX) was used to monitor cell movements within the tube. A video camera (model NC-70; Dage-MTI Inc., Wabash, MI) was attached to the microscope, and a continuous record of cell migration was produced by a time-lapse video recorder (JVC, BR-9000U; Opto-Systems, Inc., Jenkintown, PA) at 1/60th the normal video frame rate (i.e., 30 frames/min). In addition, digitized still images of the field of view were collected on the computer at 1.5-min intervals for 13.5 min. In preliminary experiments, cells were viewed over longer periods of time. As judged by continual motile activity, there was no loss of cell viability during 30 min on the microscope stage.

Data analysis. Subsequent to each experiment, the digitized images and accompanying video tape segment were reviewed simultaneously. During this process, the individual movements of 10 to 20 cells were roughly sketched on an overhead transparency overlying the video monitor. Using the transparency sketch as a guide, the position of each cell was accurately determined on each digitized image by outlining the cell boundary and calculating its centeroid. This procedure produced an (x, y) record of cell position at discrete intervals over a period of time. A cell was excluded from the analysis if it either (*a*) left the field of view or (*b*) did not move more than a cell radius from its initial position during an experiment. (In all of the experiments reported here, a cell never left the field of view by migrating out of the focal depth of the microscope objective during the 13.5-min observation period.) To gather information about a larger population of cells, the (x, y) records of cell movement from six individual experiments were collectively examined.

The data were analyzed as though the cells were confined to move on a two-dimensional surface: i.e., movements in the orthogonal direction were ignored. For each cell, square displacements were calculated for every possible time interval. For example, the (x, y) position of a typical cell was located every 1.5 min for a total of 13.5 min. For this cell, there were nine 1.5-min intervals, eight 3.0-min intervals, seven 4.5-min intervals, etc. For each of these 45-time intervals, a corresponding square displacement was calculated as:

$$D^2(t_i) = (x_n - x_i)^2 + (y_n - y_i)^2$$
$$n = \Phi + 1, \Phi + 2, \ldots N$$
$$i = n - \Phi = 1, 2, \ldots N - \Phi, \quad (1)$$

where $D^2(t_i)$ is the square displacement of an individual cell corresponding to the t_i time interval, N is the total number of images analyzed for a given cell (in all cases reported here, $N = 10$), n is the picture number of an image in a series of pictures ($1 < n \leq N$), (x_n, y_n) is the position of the cell in the nth image, and Φ is a dimensionless time allowing each time interval to be represented by an integer between 1 and $N - 1$ ($\Phi = t_i/t_{min}$, where t_{min} is the smallest time interval, here $t_{min} = 1.5$ min).

For a given population of cells, the random motility coefficient (μ) and persistence time (P) were determined by comparing the entire set of measured square displacements versus time to:

$$D^2(t_i)^{2D} = 4\mu(t - P + Pe^{-t/P}). \quad (2)$$

For example, for a population of 100 cells, there were 4,500 data points from which these parameters were determined. The data were fit to Eq. 2 using a modified Gauss-Newton iterative nonlinear regression technique with minimization of the sum of the square errors.

For ease of graphical visualization, the mean square displacement of the cell population was calculated at each discrete time by averaging the square displacements of each time interval over the total number of cells:

$$\langle D^2 \rangle_t = \frac{\sum_{j=1}^{N_c} \left\{ \frac{\sum_{i=1}^{N-\Phi} D^2(t_i)}{N - \Phi} \right\}_j}{N_c}, \quad (3)$$

where $\langle D^2 \rangle_t$ is the mean square displacement of the cell population corresponding to discrete time t, $D^2(t_i)$ is the square displacement of cell j for the time interval t_i, and N_c is the total number of cells analyzed.

Computer simulation. The assay method and data analysis were evaluated using computer simulations of cell migration in three dimensions. A migratory path for each cell in a cell population was generated by numerical solution of the Langevin equation (Doob, 1942):

$$dv(t) = -\beta v(t)dt + dW(t), \quad (4)$$

where v is the cell velocity and W represents the stochastic Weiner process, Gaussian random noise with mean 0 and variance $\alpha\, dt$. This equation contains two parameters: α and β. For one-dimensional movement of a population of cells whose velocities are described by this stochastic differential equation, the mean square displacement and speed are given by (Doob, 1942):

$$\langle D^2 \rangle_t^{1D} = E\{[x(t) - x(0)]^2\} = \frac{\alpha}{\beta^3}(\beta t - 1 + e^{-\beta t}) \quad (5a)$$

$$\langle S^2 \rangle^{1D} = E\{[v(t)]^2\} = \frac{\alpha}{2\beta} \quad (6a)$$

where x is the cell position and $E[\cdot]$ is the expected value. Mean square displacement and speed for two- and three-dimensional movement are obtained from Eq. 5a and 6a by the Pythagorean theorem, assuming that movement in each dimension is independent:

$$\langle D^2\rangle_t^{2D} = \langle D^2\rangle_t^{1D} + \langle D^2\rangle_t^{1D} = 2\frac{\alpha}{\beta^3}(\beta t - 1 + e^{-\beta t}) \tag{5b}$$

$$\langle D^2\rangle_t^{3D} = \langle D^2\rangle_t^{1D} + \langle D^2\rangle_t^{1D} + \langle D^2\rangle_t^{1D} = 3\frac{\alpha}{\beta^3}(\beta t - 1 + e^{-\beta t}) \tag{5c}$$

$$\langle S^2\rangle^{2D} = \langle S^2\rangle^{1D} + \langle S^2\rangle^{1D} = \frac{\alpha}{\beta} \tag{6b}$$

$$\langle S^2\rangle^{3D} = \langle S^2\rangle^{1D} + \langle S^2\rangle^{1D} + \langle S^2\rangle^{1D} = \frac{3\alpha}{2\beta}. \tag{6c}$$

It is more convenient to replace α and β with two different physical parameters: the root mean square (rms) speed, $S_n = \sqrt{\langle S^2\rangle^{nD}}$, and persistence time, $P = 1/\beta$ (Stokes, 1989):

$$\langle D^2\rangle_t = 2(S_n)^2 P(t - P + Pe^{-t/P}). \tag{7}$$

Finally, the random motility coefficient μ is defined:

$$\mu = \frac{\alpha}{2\beta^2} = \frac{(S_n)^2 P}{n} \tag{8}$$

so that the expressions for mean square displacement reduce to:

$$\langle D^2\rangle_t^{1D} = 2\mu(t - P + Pe^{-t/P}) \tag{9a}$$

$$\langle D^2\rangle_t^{2D} = 4\mu(t - P + Pe^{-t/P}) \tag{9b}$$

$$\langle D^2\rangle_t^{3D} = 6\mu(t - P + Pe^{-t/P}). \tag{9c}$$

It is important to notice that (*a*) the value of rms speed for a cell population depends on the dimensionality (Eq. 6), (*b*) the value of the random motility coefficient does not depend on dimensionality (Eq. 8), and (*c*) as t gets large, the mean square displacements predicted by this model are identical to those predicted by one-, two-, and three-dimensional random walks (Berg, 1983).

Our method of simulation, based on numerical integration of Eq. 4, is a three-dimensional extension of the simulations previously implemented by Lauffenburger, Tranquillo, and Stokes (Tranquillo, 1986; Stokes, 1989). The simulation was initiated by generating a uniform cell dispersion within a cubic volume element ($L \times L \times L$), where the (x, y, z) position of each cell was randomly assigned from a uniform distribution. Each cell was also assigned an initial velocity (v_x, v_y, v_z); each component was independently and randomly assigned from a Gaussian distribution with mean 0 and variance $\alpha(\Delta t)$, where Δt is the time step size used in the numerical simulation. The simulation proceeded in small time steps, where the position and velocity of each cell in the dispersion were updated at each time step:

$$\frac{x'}{S_2P} = \frac{x}{S_2P} + \frac{v_x}{S_2}\Delta t; \quad \frac{y'}{S_2P} = \frac{y}{S_2P} + \frac{v_y}{S_2}\Delta t; \quad \frac{z'}{S_2P} = \frac{z}{S_2P} + \frac{v_y}{S_2}\Delta t \tag{10}$$

$$\frac{v_x'}{S_2} = \frac{v_x\Delta t}{S_2P} + \sqrt{\frac{\Delta t}{P}}G_1; \quad \frac{v_y'}{S_2} = \frac{v_x\Delta t}{S_2P} + \sqrt{\frac{\Delta t}{P}}G_2; \quad \frac{v_y'}{S_2} = \frac{v_x\Delta t}{S_2P} + \sqrt{\frac{\Delta t}{P}}G_3, \tag{11}$$

where (x, y, z) and (v_x, v_y, v_z) are components of the cell position and velocity vectors before the time step, (x', y', z') and (v_x', v_y', v_z') are the components of the cell position and velocity vectors after the time step, the G_is are random numbers selected from a Gaussian distribution with mean 0 and variance 1. Values of μ and P were selected to approximate the experimental results. The rms speed for the nondimensionalization, S_2, was uniquely determined by selection of μ and P (Eq. 8). The step size ($\Delta t = 0.1$ s) was selected according to previously published criteria (Stokes, 1989). In preliminary simulations, the step size was incrementally decreased to insure that it was small enough to permit an accurate calculation.

The simulation described above yielded a three-dimensional path for each cell in the dispersion over a specific period of time. Because our microscopic observations were limited to a volume corresponding to the depth of focus of the microscope objective, our laboratory experiments resulted in a two-dimensional projected path for each cell in a dispersion (Fig. 1). To simulate our experimental measurements, we calculated square displacements for every possible time step (corresponding to our experimental time intervals, i.e., 1.5, 3.0, 4.5 min, etc.) for each cell in the simulated dispersion, using either (*a*) the three-dimensional cell paths:

$$D^2(t_i)^{3D} = (x_n - x_i)^2 + (y_n - y_i)^2 + (z_n - z_i)^2$$
$$n = \Phi + 1, \Phi + 2, \ldots N$$
$$i = n - \Phi = 1, 2, \ldots N - \Phi \tag{12}$$

or (*b*) the projected cell paths in a hypothetical field of view:

$$D^2(t_i)^{2D} = (x_n - x_i)^2 + (y_n - y_i)^2$$
$$n = \Phi + 1, \Phi + 2, \ldots N$$
$$i = n - \Phi = 1, 2, \ldots N - \Phi \tag{13}$$

with variables defined as in Eq. 1.

The square displacements generated from the two-dimensional cell paths (Eq. 13) were compared with those predicted by Eq. 2 (or 9b). The three-dimensional square displacements (Eq. 12) were compared with those predicted by the three-dimensional analogue of Eq. 2 (Eq. 9c). Exactly as in the experimental data analysis, the parameters μ and P were determined by fitting the simulated data to the appropriate equation using nonlinear regression with minimization of the sum of the square errors. Mean square displacements were also calculated using Eq. 3.

RESULTS

Computer simulations of cell migration

In the experiments reported here, we monitered cell migration through a three-dimensional environment by viewing two-dimensional projections with a depth of focus ~5× larger than a cell diameter. The extension of

previous analytical techniques to this specialized case was not obvious. Therefore, we used computer simulations to validate our methods of data analysis. The validity of our general approach, using a stochastic model of persistent random walks (Eq. 4) to generate cell migratory paths, has been established by previous investigators using fibroblasts (Dunn and Brown, 1987), white blood cells (Tranquillo, 1986), and endothelial cells (Stokes, 1989). By selecting input parameters (the random motility coefficient (μ) and persistence time (P)) the characteristics of the simulation were matched to the cells used in our laboratory experiments. To estimate the accuracy of our data analysis methods, and to aid in experimental design, we monitored the progress of our simulations in exactly the same way we monitored the progress of our experiments.

The computer simulations produced migratory cell paths that appeared similar to the three-dimensional paths of Brownian particles (Fig. 2). Mean square displacements calculated from these paths (Eq. 3) increase with time as expected for a persistent random walk (Fig. 3). As the number of cells in the simulation increased, the population behavior more closely approximated that predicted by solution of the Langevin equation (Fig. 3). To quantify this behavior, and to estimate the minimum number of cell observations necessary to assure accurate prediction of population behavior, random motility coefficients and persistence times were estimated by fitting square displacements calculated from the simulated cell paths to appropriate two- or three-dimensional models (Fig. 4). When only a few cells were observed ($N_{cells} = 10$), the variability in the estimates of μ and P was high, particularly for estimates from two-dimensional projections (Fig. 4, *b* and *d*). However, all the parameter estimates for $N_{cells} \geq 50$ were close to the actual population values, suggesting that experiments involving a relatively small number of cells were appropriate for predicting population behavior. Based on these results, we monitored the movements of ~100 cells in each of our quantitative experiments.

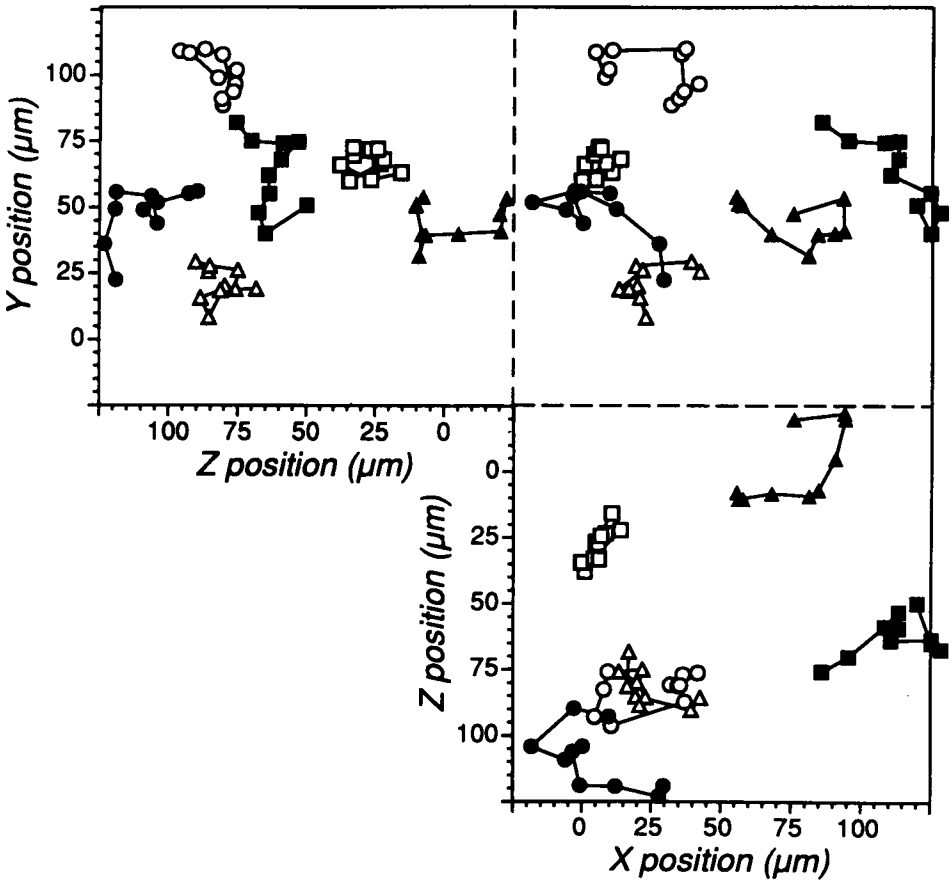

FIGURE 2 Random paths of cells generated by computer simulation (Eqs. 10 and 11). Projections of three-dimensional cell paths on three orthogonal reference planes are shown for six cells simulated using $\mu = 4.3 \times 10^{-9}$ cm^2/s and $P = 0.5$ min. Each cell path represents a total simulation time of 13.5 min; the simulation time elapsed between each symbol was 1.5 min.

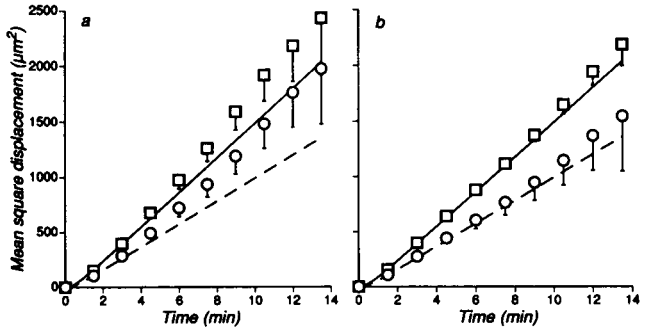

FIGURE 3 Mean square displacement versus time for cell paths generated by computer simulation using 20 cells (*a*) or 100 cells (*b*). Three-dimensional cell paths were generated as in Fig. 2. The mean square displacement (Eq. 3) is plotted versus time for the complete three-dimensional cell path (□) or a two-dimensional projection (○); error bars indicate the standard error of the mean, shown only on one side of the symbol. The solid line indicates the predicted three-dimensional behavior (Eq. 9c), and the dashed line indicates the predicted two-dimensional behavior (Eq. 9b), assuming the parameter values input to the simulation ($\mu = 4.3 \times 10^{-9}$ cm²/s and $P = 0.5$ min).

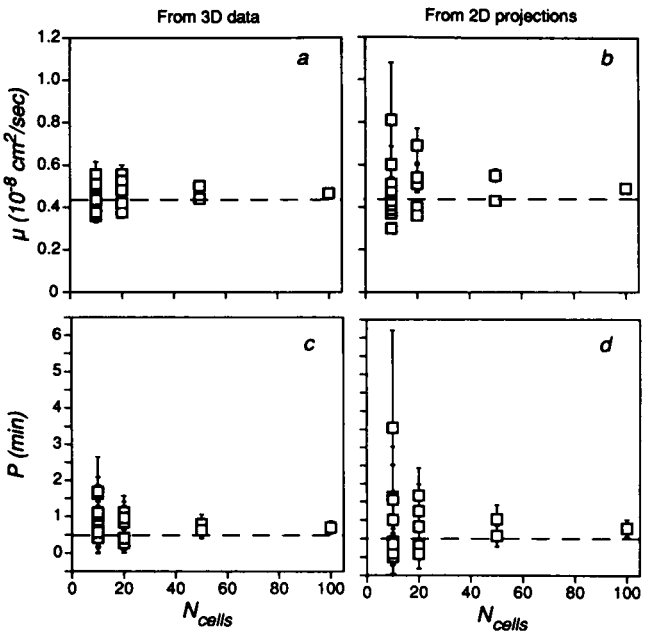

FIGURE 4 Variation of parameter estimates with the number of cells in the population. Three-dimensional cell paths were generated as in Fig. 2. Square displacements were calculated from these paths (Eq. 12) or by projections of these paths onto a two-dimensional plane (Eq. 13) and compared with models based on solutions to the stochastic differential equation. Random motility coefficients (*a*) and persistence times (*b*) were estimated by nonlinear regression of the complete three-dimensional data to the corresponding model (Eq. 9c). Random motility coefficients (*c*) and persistence times (*d*) were also estimated by nonlinear regression of the reduced (projected) data set to the two-dimensional model (Eq. 9b). Symbols represent parameter estimates, and error bars indicate the asymptotic standard error. Where not apparent, the error bar was smaller than the symbol.

Collagen preparation and characterization

Collagen was extracted from the tendons of rat tails according to established methods. As determined by lyophilization and protein assay, the collagen concentrations of stock solutions ranged from 1 to 3 mg/ml. No major impurities were detected by SDS-PAGE, and the banding pattern was identical to that of commercially-available type I collagen solutions. Furthermore, the banding pattern of collagen in the 0.02 M acetic acid stock solution remained unchanged after 8 mo of storage at 4°C.

In previous experiments, we examined the structure of collagen gels with varying amounts of collagen by scanning electron microscopy (Saltzman et al., 1992). Over the range of interest for the current experiments, the structure of the gels was similar at all concentrations, consisting of randomly arranged fibers of ~0.15 μm diameter. The gels were prepared for microscopy by dehydration through a series of ethanol solutions followed by critical point drying with liquid CO_2. Assuming this dehydration induces a considerable amount of sample shrinkage (10–40% linear), the inter-fiber spacing in the 0.1 mg/ml collagen gel was estimated to be on the order of 5 μm. As the collagen concentration was increased to 0.6 mg/ml, this spacing decreased.

Cell migration in collagen gels

The pattern of individual cell movement within the collagen gels (Fig. 5) was strikingly similar to the pattern of movement predicted by our computer simulations (Fig. 2). The dramatic difference between cell movement in gels with different collagen concentration is apparent in the pattern of movement of only a few randomly selected cells (compare the distance traveled by cells in Fig. 5 *a* to *b*). The effect of collagen gel hydration on cell movement was examined by quantifying cell motility in neutrophil-populated gels differing only in the concentration of collagen. For each collagen concentration, six individual experiments, involving 10 to 20 cells each, were performed. The results from the six experiments at a given collagen concentration were collectively analyzed (Fig. 6). A random motility coefficient and persistence time were estimated from each set of experimental data (square displacement versus time) by nonlinear regression (Fig. 7 and Table 1). Similar to previous studies of cell motility on two-dimensional surfaces (Farrell et al., 1990), the errors associated with

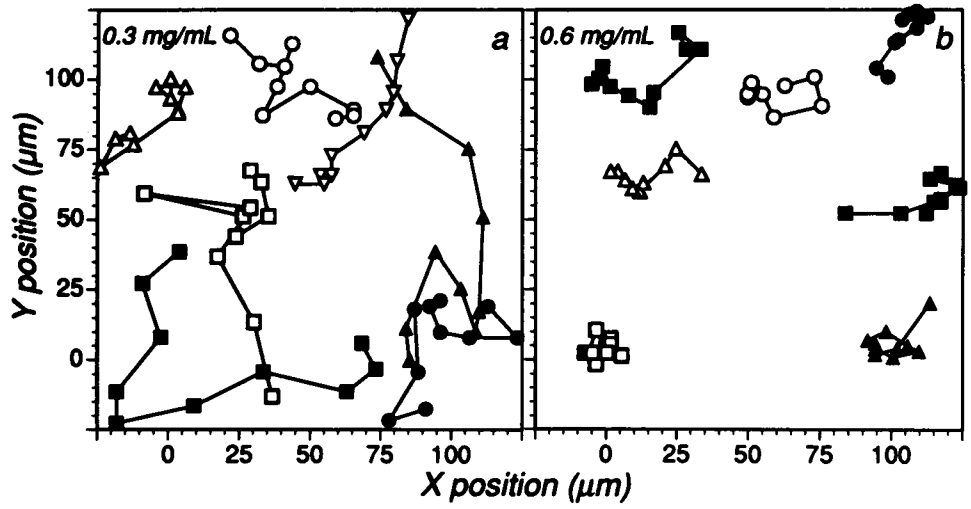

FIGURE 5 Two-dimensional projection of sample cell paths for human neutrophils migrating in a three-dimensional gel of rat tail collagen at (*a*) 0.3 mg/ml and (*b*) 0.6 mg/ml. Each cell path (indicated by a different symbol) represents a total measurement time of 13.5 min; the time elapsed between each symbol was 1.5 min.

the estimates of persistence time preclude any absolute statements about the relationship between collagen concentration and persistence. However, the random motility coefficient changed by nearly a factor of 10 over a relatively narrow range of concentration with a maximum at 0.3 mg/ml.

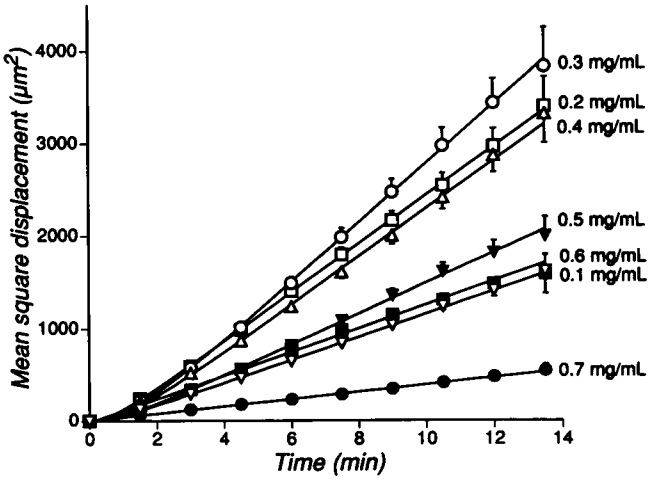

FIGURE 6 Mean square displacement versus time for human neutrophils migrating in three dimensional gels of rat tail collagen with varying hydration (0.1 to 0.7 mg/ml). For each experiment at a different collagen concentration, between 89 and 120 cells were tracked at 1.5-min intervals for 13.5 min. The solid lines, obtained by nonlinear regression, indicate the best fit of the experimental data to Eq. 2 (see Table 1).

DISCUSSION

From our earliest experiments for this report, it was clear that human neutrophils move rapidly within three-dimensional gels of rat tail collagen, and that the rate of movement depends on the nature of the surrounding gel. This observation may have important implications. In fulfilling their role in the immune response, neutro-

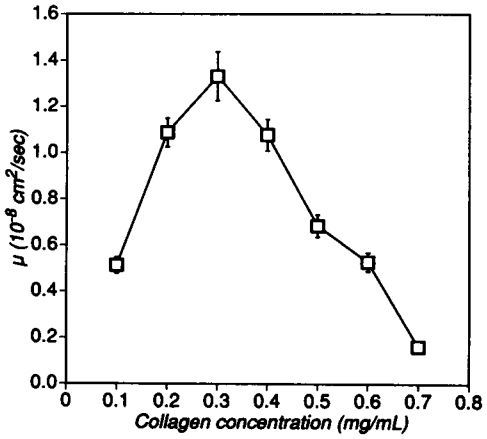

FIGURE 7. Random motility coefficient (μ) versus collagen concentration for human neutrophils migrating in three-dimensional rat tail collagen gels. Values of the random motility coefficient were obtained by nonlinear regression, and error bars represent 95% confidence limits. This figure is a graphical representation of a portion of the data presented in Table 1.

TABLE 1 **Random motility coefficient (μ) and persistence time (P) for human neutrophils migrating in rat tail collagen**

Collagen concentration in gel	μ	P	N_{cells}
mg/ml	10^{-9} *cm²/s*	*min*	
0.1	5.1 ± 0.4	0.7 ± 0.4	120
0.2	10.9 ± 0.6	0.7 ± 0.4	100
0.3	13.3 ± 1.1	1.3 ± 0.5	95
0.4	10.8 ± 0.7	1.2 ± 0.4	105
0.5	6.9 ± 0.5	1.0 ± 0.5	115
0.6	5.3 ± 0.4	0.2 ± 0.5	89
0.7	1.6 ± 0.1	0.0 ± 0.5	91

The indicated values for μ and *P* are the best estimates, obtained by nonlinear regression, ±95% confidence limit.

phils migrate out of capillaries, through tissue, to sites of infection. Perhaps in tissues, cell speed is influenced by the level of ECM hydration, as we have shown here in vitro. The local tissue edema that accompanies inflammation may be a significant factor modulating the rate of neutrophil infiltration. Similar factors may influence the speed of leukocyte migration (and therefore the efficiency of immune cell surveillance) in mucus secretions. For these reasons, we developed experimental techniques for quantifying cell movement in three-dimensional gels, as a first step in evaluating the mechanism by which cells migrate through tissues.

The similarity between trajectories of motile cells and particles undergoing Brownian motion is striking (Fig. 5), suggesting that diffusion might be responsible for the movement we have quantified. The diffusion coefficient for a spherical particle in water can be estimated from the Stokes-Einstein equation:

$$D_w = \frac{kT}{6\pi\eta r}, \tag{14}$$

where D_w is the diffusion coefficient of the particle in water, k is Boltzman's constant, T is the absolute temperature, η is the viscosity of water at T, and r is the radius of the particle. For a particle with a radius of 5 μm diffusing in water at 37°C, Eq. 14 gives D_w of 6×10^{-10} cm²/s, not much lower than the smallest random motility coefficient measured with our experimental system (i.e., 16×10^{-10} cm²/s). We have noticed, however, that red blood cells, which are similar in size to neutrophils, never moved during our experiments, even when the experimental duration was 30 min. Furthermore, if diffusion was responsible for cell movement, the diffusion coefficient would monotomically decrease with increasing collagen concentration due to the increase in viscosity and/or viscoelasticity; however, we measured a maximum in the random motility coefficient at an intermediate collagen concentration. Based on these observations we believe that the fibers in the gel prevent diffusion of cell-sized particles; there must be some active interaction between neutrophils and collagen fibers enabling these cells to traverse the gel.

Random motility coefficients for human neutrophils within gels of rat tail collagen varied from 1.6 to 13×10^{-9} cm²/s (Table 1). Two alternative quantitative assays have been previously employed to estimate this coefficient for neutrophils. Using an under-agarose assay, in which cells are attached to a two-dimensional substrate, μ was $\sim 10^{-8}$ cm²/s (Lauffenburger, 1983), near the maximum observed in this study; using a filter assay, where cells migrate through a three-dimensional mesh of synthetic fibers, μ was $\sim 10^{-9}$ cm²/s (Buettner et al., 1989), near our minimum. While there are potentially important quantitative differences between observed migration rates in these assay systems, it is interesting that these three very different techniques yield similar values for the random motility coefficient.

Several previous reports examining the relationship between adhesion and cell motility on surfaces suggest that the strength of a cell-surface adhesion must be at an optimal level for cell migration (Lackie, 1986; DiMilla et al., 1991; Saltzman et al., 1991). If the adhesive strength is well above this optimum, cells will become fixed to the surface, and hence, will not migrate. If cell-surface adhesion falls much below the optimal level, the cell will not be able to gain sufficient traction to translocate across the surface. Our results are consistent with an optimal adhesiveness for neutrophils migrating in three-dimensional collagen gels. Below a concentration of 0.1 mg/ml, most cells rapidly sank through the gel; at concentrations above 0.7 mg/ml, the majority of neutrophils were immobilized (although neutrophils were seen to extend and retract pseudopodia in these high concentration gels, they were unable to make significant displacements from their initial positions). Between these two extremes, neutrophils exhibited maximal motility at a collagen concentration of 0.3 mg/ml (Fig. 7). Inter-collagen fiber spacing is approximately equal to a neutrophil diameter (~ 10 μm) at 0.1 mg/ml, and decreases as the collagen concentration is raised (Saltzman et al., 1992). Our results suggest that when the collagen concentration is increased above the optimal level (0.3 mg/ml), the strength of the cell-fiber interactions becomes stronger due to the increased number of collagen fibers surrounding the cell. Analogously, at lower collagen concentrations, where there are fewer fibers, the cell-fiber adhesive strength is lower. Both of these situations result in a decrease in the effectiveness with which cells are able to migrate through the gel.

Assuming that neutrophils are able to migrate actively through collagen gels by adhesive interactions with

collagen fibers, the methods presented here can be used to investigate the nature of this adhesion. In particular, a variety of factors can be added to the cell-populated collagen gels and cell motility quantified. If the cell-fiber interaction is mediated by surface receptor-ligand bonds, the addition of monoclonal antibodies against the relevent surface receptors should alter the motile behavior of the cells. Also, many extracellular matrix components are known to influence the adhesive properties of collagen (e.g., laminin and hyaluronic acid). By characterizing the motility of cells in the presence of these factors, we can gain further information about how cells migrate through more complex three-dimensional matrices like tissue.

The methods presented here are flexible. By combining different cell types with their native ECM components, this in vitro cell culture technique can be used to mimic a variety of physiological situations. For example, we have demonstrated that PC12 cells and chicken hepatocytes can be encapsulated by similar methods and that cell viability and function are retained (Saltzman et al., 1992). Furthermore, we have developed methods for releasing polypeptide growth factors from a biocompatible polymer implant into a three-dimensional cell culture system (Saltzman et al., 1992) and for establishing diffusion-limited concentration gradients of bioactive compounds in three-dimensional biological gels (Radomsky et al., 1990). By combining these experimental methods and extending our analytical treatment to include nonrandom cell behavior (Farrell et al., 1990), we can investigate chemotaxis or other dynamic gradient-induced processes underlying tissue organization and function.

We thank Professor Richard A. Cone for his critical review of this manuscript, and Professors Michael Edidin and Charles C. Clark for their helpful discussions. We also thank the referees for their comments which greatly improved the clarity of this manuscript.

Supported by grants from the National Science Foundation (EET-8815629 and BCS-9007762) and the National Institutes of Health (GM-43873). M.R. Parkhurst is a Howard Hughes Medical Institute Predoctoral Fellow. W.M. Saltzman is a Camille and Henry Dreyfus Teacher-Scholar (1990).

Received for publication 29 July 1991 and in final form 23 September 1991.

REFERENCES

Allan, R. B., and P. C. Wilkinson. 1978. A visual analysis of chemotactic and chemokinetic locomotion of human neutrophil leukocytes: use of a new assay with *Candida albicans* as gradient source. *Exp. Cell Res.* 111:191–203.

Bell, E. B., B. Ivarsson, and C. Merrill. 1979. Production of a tissue-like structure by contraction of collagen lattices by human fibroblasts of different proliferative potential in vitro. *Proc. Natl. Acad. Sci. USA.* 75:1274–1278.

Bellairs, R., A. Curtis, and G. Dunn, editors. 1982. Cell Behavior. Cambridge University Press, Cambride, UK. 615 pp.

Berg, H. C. 1983. Random Walks in Biology. Princeton University Press, Princeton, NJ. 142 pp.

Boyden, S. V. 1962. The chemotactic effect of mixtures of antibody and antigen on polymorphonuclear leukocytes. *J. Exp. Med.* 115:453–466.

Brown, A. F. 1982. Neutrophil granulocytes: adhesion and locomotion on collagen substrata and in collagen matrices. *J. Cell Sci.* 58:455–467.

Buettner, H. M., D. A. Lauffenburger, and S. H. Zigmond. 1989. Measurement of leukocyte motility and chemotaxis parameters with the Millipore filter assay. *J. Immunol. Methods.* 123:25–37.

Comandon, J. 1917. Phagocytose *in vitro* des hematozoaires du calfat (enregistrement cinematographique). *Compt. Rend. Soc. Biol. (Paris).* 80:314–316.

Cunningham, C. C., T. P. Stossel, and D. J. Kwiatkowski. 1991. Enhanced motility in NIH 3T3 fibroblasts that overexpress gelsolin. *Science (Wash. DC).* 251:1233–1236.

Cutler, J. 1974. A simple *in vitro* method for studies on chemotaxis. *Proc. Soc. Exp. Biol. Med.* 147:471–474.

DiMilla, P. A., K. Barbee, and D. A. Lauffenburger. 1991. Mathematical model for the effects of adhesion and mechanics on cell migration speed. *Biophys. J.* 60:15–37.

Doob, J. L. 1942. The Brownian movement and stochastic equations. *Annals of Mathematics.* 43:351–369.

Dunn, G. A. 1983. Characterizing a kinesis response: time averaged measures of cell speed and directional persistence. *Agents Actions Suppl.* 12:14–33.

Dunn, G. A., and A. F. Brown. 1987. A unified approach to analyzing cell motility. *J. Cell Sci. Suppl.* 8:81–102.

Elsdale, T., and J. Bard. 1972. Collagen substrata for studies on cell behavior. *J. Cell Biol.* 54:626–637.

English, D., and B. R. Andersen. 1974. Single-step separation of red blood cells: granulocytes and mononuclear leukocytes on discontinuous density gradient of ficoll-hypaque. *J. Immunol. Methods.* 5:249–252.

Farrell, B. E., R. P. Daniele, and D. A. Lauffenburger. 1990. Quantitative relationships between single-cell and cell-population model parameters for chemosensory migration responses of alveolar macrophages to C5a. *Cell Motil. Cytoskeleton.* 16:279–293.

Folkman, J. 1985. Toward an understanding of angiogenesis: search and discovery. *Perspect. Biol. Med.* 29:10–36.

Gail, M. H., and C. W. Boone. 1970. The locomotion of mouse fibroblasts in tissue culture. *Biophys. J.* 10:980–993.

Haston, W. S., J. M. Shields, and P. C. Wilkinson. 1982. Lymphocyte locomotion and attachment on two-dimensional surfaces and in three-dimensional matrices. *J. Cell Biol.* 92:747–752.

Haston, W. S., and P. C. Wilkinson. 1988. Visual methods for measuring leukocyte locomotion. *Methods Enzymol.* 162:17–38.

Ishihara, A., B. Holifield, and K. Jacobsen. 1988. Analysis of lateral redistribution of a monoclonal antibody complex plasma membrane glycoprotein which occurs during cell locomotion. *J. Cell Biol.* 106:329–343.

Lackie, J. M. 1986. Cell Movement and Cell Behavior. Allen and Unwin, London. 316 pp.

Lauffenburger, D. A. 1983. Measurement of phenomenological parameters for leukocyte motility and chemotaxis. *Agents Actions Suppl.* 12:34–53.

Nelson, R. D., P. G. Quie, and R. L. Simmons. 1975. Chemotaxis under agarose: a new and simple method for measuring chemotaxis and spontaneous migration of human polymorphonuclear leukocytes and monocytes. *J. Immunol.* 115:1650–1656.

Poste, G., and I. J. Fidler. 1980. The pathogenesis of cancer metastasis. *Nature (Lond.)* 283:139–146.

Radomsky, M. L., K. J. Whaley, R. A. Cone, and W. M. Saltzman. 1990. Macromolecules released from polymers: diffusion into unstirred fluids. *Biomaterials.* 11:619–624.

Richards, J., L. Larson, J. Yang, R. Guzman, Y. Tomooka, R. Osborn, W. Imagawa, and S. Nandi. 1983. Method for culturing mammary epithelial cells in a rat tail collagen gel matrix. *Journal of Tissue Culture Methods.* 8:31–36.

Saltzman, W. M., M. R. Parkhurst, P. Parsons-Wingerter, and W. H. Zhu. 1992. Three-dimensional cell cultures mimic tissues. *Ann. NY Acad. Sci.* In press.

Saltzman, W. M., P. Parsons-Wingerter, K. W. Leong, and S. Lin. 1991. Fibroblast and hepatocyte behavior on synthetic polymer surfaces. *J. Biomed. Mater. Res.* 25:741–759.

Sato, M., W. H. Schwarz, and T. D. Pollard. 1987. Dependence of the mechanical properties of actin/α-actinin gels on deformation rate. *Nature (Lond.)* 325:828–830.

Schor, S. L. 1980. Cell proliferation and migration on collagen substrate in vitro. *J. Cell Sci.* 41:159–175.

Schor, S. L., T. D. Allen, and C. J. Harrison. 1980. Cell migration through three-dimensional gels of native collagen fibres: collagenolytic activity is not required for the migration of two permanent cell lines. *J. Cell Sci.* 46:171–186.

Schor, S. L., A. M. Schor, and G. W. Bazill. 1981. The effects of fibronectin on the migration of human foreskin fibroblasts and Syrian hamster melanoma cells into three-dimensional gels of native collagen fibres. *J. Cell Sci.* 48:301–314.

Sheetz, M. P., S. Turney, H. Qian, and E. L. Elson. 1989. Nanometre-level analysis demonstrates that lipid flow does not drive membrane glycoprotein movements. *Nature (Lond.).* 340:284–288.

Stokes, C. 1989. Quantitative studies of endothelial cell motility and chemotaxis in angiogenesis. Ph.D. Thesis. University of Pennsylvania, Philadelphia. 314 pp.

Tranquillo, R. T. 1986. Phenomenological and fundamental descriptions of leukocyte random motility and chemotaxis. Ph.D. Thesis. University of Pennsylvania, Philadelphia. 319 pp.

Tranquillo, R. T., D. A. Lauffenburger, and S. H. Zigmond. 1988. A stochastic model for leukocyte random motility and chemotaxis based on receptor binding fluctuations. *J. Cell Biol.* 106:303–309.

Trinkhaus, J. P. 1984. Cells into Organs: Forces that Shape the Embryo. 2nd ed. Prentice-Hall, New Jersey. 543 pp.

Wilkinson, P. C. 1985. A Visual study of chemotaxis of human lymphocytes using a collagen-gel assay. *J. Immunol. Methods.* 76:105–120.

Wilkinson, P. C., and J. M. Lackie. 1979. The adhesion, migration and chemotaxis of leukocytes in inflammation. *In* Inflammatory Reaction. H. Z. Movat, editor. Springer-Verlag, Berlin. 47–88.

Wilkinson, P. C., J. M. Lackie, and R. B. Allan. 1982. Methods for measuring leukocyte locomotion. *In* Cell Analysis. Vol. 1. N. Catsimpoolas, editor. Plenum Press, New York. 145–194.

Wilkinson, P. C., J. M. Lackie, W. S. Haston, and L. N. Islam. 1988. Effects of phorbol esters on shape and locomotion of human blood lymphocytes. *J. Cell Sci.* 90:645–655.

Zigmond, S. H. 1977. Ability of polymorphonuclear leukocytes to orient in gradients of chemotactic factors. *J. Cell Biol.* 75:606–616.